2010

Nanometer-scale distance measurements in proteins using Gd3+ spin labeling

Alexey Potapov
Weizmann Institute of Science

Hiromasa Yagi
Australian National University

Thomas Huber
Australian National University

Slobodan Jergic
University of Wollongong, jergic@uow.edu.au

Nicholas E. Dixon
University of Wollongong, nickd@uow.edu.au

See next page for additional authors

Publication Details

Potapov, A., Yagi, H., Huber, T., Jergic, S., Dixon, N. E., Otting, G. & Goldfarb, D. (2010). Nanometer-scale distance measurements in proteins using Gd3+ spin labeling. Journal of the American Chemical Society, 132 (26), 9040-9048.

Nanometer-scale distance measurements in proteins using Gd3+ spin labeling

Abstract

Methods for measuring nanometer-scale distances between specific sites in proteins are essential for analysis of their structure and function. In this work we introduce Gd3+ spin labeling for nanometer-range distance measurements in proteins by high-field pulse electron paramagnetic resonance (EPR). To evaluate the performance of such measurements, we carried out four-pulse double-electron electron resonance (DEER) measurements on two proteins, p75ICD and τC14, labeled at strategically selected sites with either two nitroxides or two Gd3+ spin labels. In analogy to conventional site-directed spin labeling using nitroxides, Gd3+ tags that are derivatives of dipicolinic acid were covalently attached to cysteine thiol groups. Measurements were carried out on X-band (~9.5 GHz, 0.35 T) and W-band (95 GHz, 3.5 T) spectrometers for the nitroxide-labeled proteins and at W-band for the Gd3+-labeled proteins. In the protein p75ICD, the orientations of the two nitroxides were found to be practically uncorrelated, and therefore the distance distribution could as readily be obtained at W-band as at X-band. The measured Gd3+-Gd3+ distance distribution had a maximum at 2.9 nm, as compared to 2.5 nm for the nitroxides. In the protein τC14, however, the orientations of the nitroxides were correlated, and the W-band measurements exhibited strong orientation selection that prevented a straightforward extraction of the distance distribution. The X-band measurements gave a nitroxide-nitroxide distance distribution with a maximum at 2.5 nm, and the W-band measurements gave a Gd3+-Gd3+ distance distribution with a maximum at 3.4 nm. The Gd3+-Gd3+ distance distributions obtained are in good agreement with expectations from structural models that take into account the flexibility of the tags and their tethers to the cysteine residues. These results show that Gd3+ labeling is a viable technique for distance measurements at high fields that features an order of magnitude sensitivity improvement, in terms of protein quantity, over X-band pulse EPR measurements using nitroxide spin labels. Its advantage over W-band distance measurements using nitroxides stems from an intrinsic absence of orientation selection.

Keywords

distance, measurements, scale, nanometer, proteins, spin, labeling, gd3, CMMB

Disciplines

Life Sciences | Physical Sciences and Mathematics | Social and Behavioral Sciences

Publication Details

Potapov, A., Yagi, H., Huber, T., Jergic, S., Dixon, N. E., Otting, G. & Goldfarb, D. (2010). Nanometer-scale distance measurements in proteins using Gd3+ spin labeling. Journal of the American Chemical Society, 132 (26), 9040-9048.

Authors

Alexey Potapov, Hiromasa Yagi, Thomas Huber, Slobodan Jergic, Nicholas E. Dixon, Gottfried Otting, and Daniella Goldfarb

J|A|C|S
ARTICLES

Published on Web 06/10/2010

Nanometer-Scale Distance Measurements in Proteins Using Gd^{3+} Spin Labeling

Alexey Potapov,[#] Hiromasa Yagi,[†] Thomas Huber,[†] Slobodan Jergic,[‡] Nicholas E. Dixon,[‡] Gottfried Otting,*[,†] and Daniella Goldfarb*[,#]

Department of Chemical Physics, Weizmann Institute of Science, Rehovot, 76100, Israel, Research School of Chemistry, The Australian National University, Canberra ACT 0200, Australia, and School of Chemistry, University of Wollongong, NSW 2522, Australia

Received February 23, 2010; E-mail: daniella.goldfarb@weizmann.ac.il; go@rsc.anu.edu.au

Abstract: Methods for measuring nanometer-scale distances between specific sites in proteins are essential for analysis of their structure and function. In this work we introduce Gd^{3+} spin labeling for nanometer-range distance measurements in proteins by high-field pulse electron paramagnetic resonance (EPR). To evaluate the performance of such measurements, we carried out four-pulse double-electron electron resonance (DEER) measurements on two proteins, p75ICD and τ_C14, labeled at strategically selected sites with either two nitroxides or two Gd^{3+} spin labels. In analogy to conventional site-directed spin labeling using nitroxides, Gd^{3+} tags that are derivatives of dipicolinic acid were covalently attached to cysteine thiol groups. Measurements were carried out on X-band (~9.5 GHz, 0.35 T) and W-band (95 GHz, 3.5 T) spectrometers for the nitroxide-labeled proteins and at W-band for the Gd^{3+}-labeled proteins. In the protein p75ICD, the orientations of the two nitroxides were found to be practically uncorrelated, and therefore the distance distribution could as readily be obtained at W-band as at X-band. The measured Gd^{3+}–Gd^{3+} distance distribution had a maximum at 2.9 nm, as compared to 2.5 nm for the nitroxides. In the protein τ_C14, however, the orientations of the nitroxides were correlated, and the W-band measurements exhibited strong orientation selection that prevented a straightforward extraction of the distance distribution. The X-band measurements gave a nitroxide–nitroxide distance distribution with a maximum at 2.5 nm, and the W-band measurements gave a Gd^{3+}–Gd^{3+} distance distribution with a maximum at 3.4 nm. The Gd^{3+}–Gd^{3+} distance distributions obtained are in good agreement with expectations from structural models that take into account the flexibility of the tags and their tethers to the cysteine residues. These results show that Gd^{3+} labeling is a viable technique for distance measurements at high fields that features an order of magnitude sensitivity improvement, in terms of protein quantity, over X-band pulse EPR measurements using nitroxide spin labels. Its advantage over W-band distance measurements using nitroxides stems from an intrinsic absence of orientation selection.

Introduction

Methods for distance measurements between specific sites in biomolecules (proteins and nucleic acids) and their assemblies are essential for structural studies that resist the application of X-ray crystallography and solution NMR spectroscopy, such as membrane proteins in their native environment and large biomolecular complexes. One such method, which has become increasingly popular in recent years, is pulse electron paramagnetic resonance (EPR) spectroscopy.[1−6] It requires two or more paramagnetic centers with unpaired electrons and can measure distances between them in the range of 1.5−8 nm. The measurement is based on the dipolar interaction, ω_{dd}, between two unpaired electrons that is given by

$$\omega_{dd} = c/r^3 \quad (1)$$

where r is the distance between the two electrons and c is a known constant. The most popular technique for measuring the frequency ω_{dd} is the four-pulse double-electron electron resonance (DEER) sequence[7] shown in Figure 1a. Because most biomolecules do not contain paramagnetic centers naturally, they are usually introduced by attaching nitroxide radicals. In proteins this can be achieved through modification of each of two cysteine residues using 1-oxyl-2,2,5,5-tetramethylpyrroline-3-methyl methanethiosulfonate (MTSL) (Figure 1b).[8−10] The

[#] Weizmann Institute of Science.
[†] The Australian National University.
[‡] University of Wollongong.

(1) Milov, A. D.; Ponomarev, A. B.; Tsvetkov, Y. D. *Chem. Phys. Lett.* **1984**, *110*, 67–72.
(2) Borbat, P. P.; Freed, J. H. *Methods Enzymol.* **2007**, *423*, 52–116.
(3) Schiemann, O.; Prisner, T. F. *Q. Rev. Biophys.* **2007**, *40*, 1–53.
(4) Banham, J. E.; Baker, C. M.; Ceola, S.; Day, I. J.; Grant, G. H.; Groenen, E. J. J.; Rodgers, C. T.; Jeschke, G.; Timmel, C. R. *J. Magn. Reson.* **2008**, *191*, 202–218.
(5) Jeschke, G. *Chem. Phys. Chem* **2002**, *3*, 927–932.
(6) Jeschke, G.; Polyhach, Y. *Phys. Chem. Chem. Phys.* **2007**, *9*, 1895–1910.
(7) Pannier, M.; Veit, S.; Godt, A.; Jeschke, G.; Spiess, H. W. *J. Magn. Reson.* **2000**, *142*, 331–340.
(8) Hubbell, W. L.; Altenbach, C. *Curr. Opin. Struct. Biol.* **1994**, *4*, 566–573.
(9) Fanucci, G. E.; Cafiso, D. S. *Curr. Opin. Struct. Biol.* **2006**, *16*, 644–653.

10.1021/ja1015662

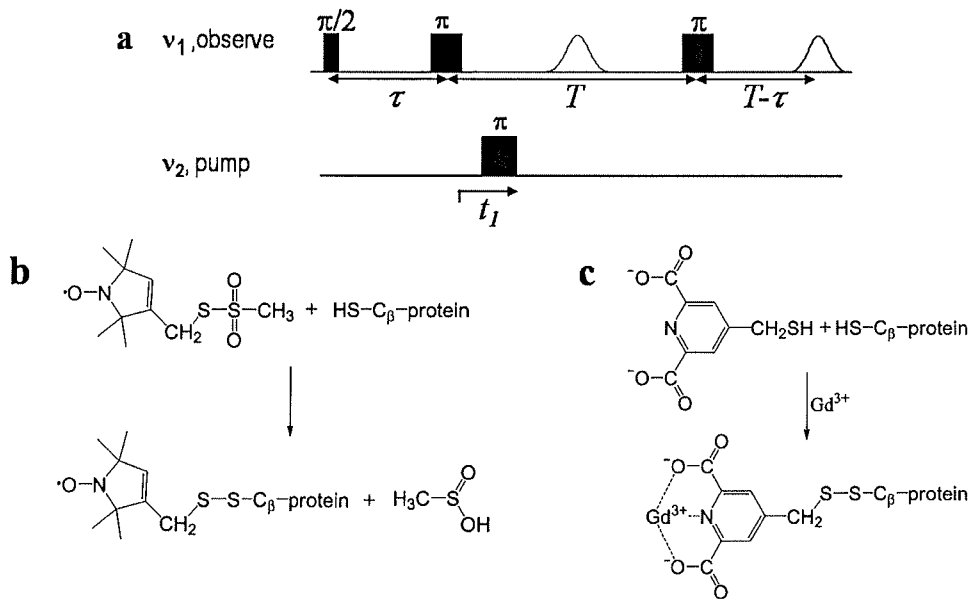

Figure 1. (a) The four-pulse DEER sequence used. (b) Scheme showing protein labeling with MTSL by attachment to a cysteine residue. (c) Scheme showing protein labeling with 4MMDPA by attachment to a cysteine residue and Gd^{3+} coordination. The Gd^{3+} is also coordinated to water molecules from the solvent that are not shown.

cysteines can be native or introduced at specific locations by site-directed mutagenesis.

For a pair of nitroxide radicals, each having a spin $S = 1/2$, the time evolution of the echo intensity $V(t)$ in the four-pulse DEER experiment is proportional to

$$V(t) \propto 1 - \lambda(1 - \int_0^{\pi} \int_0^{\infty} \cos(\omega_{dd}(3\cos^2\theta - 1)t) f(r)\, d\theta\, dr) \quad (2)$$

where λ is the probability to flip the electron spin by the pump pulse, $f(r)$ is the pair distance distribution, and θ is the angle between the interspin vector $\boldsymbol{r}$ and the direction of the external magnetic field. The DEER distance measurements are commonly carried out on frozen solutions at low temperatures to slow electron spin relaxation rates, using X-band pulse EPR spectrometers (i.e., operating at a microwave (mw) frequency of about 9.5 GHz and a magnetic field strength of about 0.35 T).[11–13] The spectral properties of nitroxides at X-band frequencies are such that, under appropriate positioning of the pump and observe pulses (see Figure 1a), all possible molecular orientations θ contribute to the DEER effect. In this situation, λ can be taken as orientation independent, making the integration over θ and the extraction of the desired distance distribution $f(r)$ straightforward.[14–17]

The amount of sample required for X-band DEER measurements is 30–80 μL of at least 0.1 mM solutions of doubly labeled molecules. This is a relatively large quantity that can be difficult to obtain for many proteins or nucleic acids, limiting the applicability of the method. One way to reduce the amount of sample needed is to carry out the measurements at higher frequencies.[18,19] The sensitivity of early W-band (95 GHz, 3.5 T) DEER measurements on a nitroxide biradical model compound carried out on a commercial spectrometer was severely compromised by the limited mw power available.[20] Recent measurements on home-built spectrometers, however, showed that the sensitivity could be increased dramatically by the use of increased mw power, allowing DEER measurements on as little as 2–3 μL of 0.1 mM solutions[21] or ~200 μL of 1 μM solutions.[22] This corresponds to an order of magnitude improvement in sensitivity in terms of the amount of sample needed compared with X-band measurements.

At high fields, however, the g-anisotropy of nitroxide spin labels becomes resolved so that the mw pulses can select only a limited set of molecular orientations at any given field within the EPR spectrum because of mw power limitations. While eq 2 is valid in general, orientation selection leads to orientation-dependent λ, and a nontrivial integration over θ is required. The relative orientations of the two nitroxides must be included in the analysis, and a series of DEER measurements at several magnetic fields positions along the EPR spectrum becomes

(10) Hubbell, W. L.; Gross, A.; Langen, R.; Lietzow, M. A. *Curr. Opin. Struct. Biol.* **1998**, *8*, 649–656.
(11) Schiemann, O.; Piton, N.; Plackmeyer, J.; Bode, B. E.; Prisner, T. F.; Engels, J. W. *Nature Protoc.* **2007**, *2*, 904–923.
(12) Cai, Q.; Kusnetzow, A. K.; Hideg, K.; Price, E. A.; Haworth, I. S.; Qin, P. Z. *Biophys. J.* **2007**, *93*, 2110–2117.
(13) Fafarman, A. T.; Borbat, P. P.; Freed, J. H.; Kirshenbaum, K. *Chem. Commun.* **2007**, 377–379.
(14) Jeschke, G.; Chechik, V.; Ionita, P.; Godt, A.; Zimmermann, H.; Bahman, J.; Timmel, C. R.; Hilger, D.; Jung, H. *Appl. Magn. Reson.* **2006**, *30*, 473–498.
(15) Jeschke, G.; Panek, G.; Godt, A.; Bender, A.; Paulsen, H. *Appl. Magn. Reson.* **2004**, *26*, 223–244.
(16) Jeschke, G.; Koch, A.; Jonas, U.; Godt, A. *J. Magn. Reson.* **2002**, *155*, 72–82.
(17) Sale, K.; Song, L. K.; Liu, Y. S.; Perozo, E.; Fajer, P. *J. Am. Chem. Soc.* **2005**, *127*, 9334–9335.
(18) Denysenkov, V. P.; Biglino, D.; Lubitz, W.; Prisner, T. F.; Bennati, M. *Angew. Chem., Int. Ed.* **2008**, *47*, 1224–1227.
(19) Denysenkov, V. P.; Prisner, T. F.; Stubbe, J.; Bennati, M. *Proc. Natl. Acad. Sci. U.S.A.* **2006**, *103*, 13386–13390.
(20) Polyhach, Y.; Godt, A.; Bauer, C.; Jeschke, G. *J. Magn. Reson.* **2007**, *185*, 118–129.
(21) Goldfarb, D.; Lipkin, Y.; Potapov, A.; Gorodetsky, Y.; Epel, B.; Raitsimring, A. M.; Radoul, M.; Kaminker, I. *J. Magn. Reson.* **2008**, *194*, 8–15.
(22) Cruickshank, P. A. S.; Bolton, D. R.; Robertson, D. A.; Hunter, R. I.; Wylde, R. J.; Smith, G. M. *Rev. Sci. Instrum.* **2009**, *80*, 103102.

necessary to extract $f(r)$.[20,23−25] This considerably increases the measurement time. Such an analysis has been carried out on several macromolecules with immobilized ordered intrinsic radicals.[18,19,23] MTSL-derived nitroxide labels, however, can be disordered to varying extents. When the two labels are highly disordered, there is no correlation between the orientations of the two nitroxides, the orientation selection can be ignored, and the distance distribution can be extracted from a single DEER measurement just like at X-band.[20] When the nitroxides are, however, only partially disordered, the distribution of the relative orientations of the two nitroxides renders the analysis of the DEER traces highly complex, and it becomes model dependent.[25] Moreover, the orientation information gathered from orientation-selective DEER data may have only a limited interest in the case of nitroxide-labeled proteins. Thus, alternative spin labels that provide high sensitivity at high fields and are free from orientation selection effects are called for. In this work we show that Gd^{3+} spin labels fulfill these criteria and can serve as an alternative to nitroxide spin labels for high-sensitivity distance measurements in proteins.

Gd^{3+} is a $S = 7/2$ ion with an isotropic g-factor. Its spin is closely localized on the Gd^{3+} atom, and the zero-field-splitting (ZFS) parameter D is relatively small in most complexes ($D <$ 40 mT).[26] Gd^{3+} offers a number of critical advantages over nitroxide radicals at high fields: (i) The width of the subspectrum of the central $|-1/2\rangle \leftrightarrow |1/2\rangle$ transition, δ, narrows with increasing ν_0 ($\delta \propto D^2/\nu_0$),[27] (for $\nu_0 > 32$ GHz) where ν_0 is the spectrometer frequency. Therefore, the EPR sensitivity of Gd^{3+} increases with increasing magnetic field strength, whereas the spectrum of nitroxides broadens with increasing field strength. (ii) The high spin of the Gd^{3+} ion leads to an about 4-fold larger effective amplitude of the irradiating mw field B_1 for the central transition of Gd^{3+} compared to nitroxides because of the higher transition probability. This allows applying short pump pulses also on spectrometers with limited mw power. (iii) The spin−lattice relaxation time of Gd^{3+} is short compared to those of nitroxides, allowing rapid signal averaging at cryogenic temperatures. (iv) Most importantly, the central transition, as well as the other transitions, can be considered as effectively isotropic with respect to the ligand orientation because the large ZFS distribution (in amplitude and orientation)[26] abolishes the orientation selection. The feasibility of 95 and 33 GHz (Ka-band) distance measurements between two Gd^{3+} ions has been recently demonstrated using a simple rigid bis-Gd^{3+} complex.[28] The results showed that the Gd^{3+} ion can be treated as an effective $S = 1/2$ system and that DEER data can be analyzed accordingly. Another DEER study on a highly flexible bis-Gd^{3+} complex has been recently reported.[29]

In the present work we introduce Gd^{3+} spin labeling of proteins for nanometer-range distance determination at high magnetic fields and demonstrate its potential as a viable and highly sensitive method. Different tag molecules that bind lanthanides and can be attached to the thiol group of a cysteine residue via a disulfide bond have recently been developed. While these tags were originally developed for paramagnetic NMR,[30,31] they can equally be used for Gd^{3+} spin labeling for EPR applications. As in conventional site-directed spin labeling, the Gd^{3+} is site-specifically attached to the protein by tags that are covalently attached to cysteine thiol groups (Figure 1c). For demonstration, we used two proteins labeled at selected sites with either two nitroxides or two Gd^{3+} labels. The proteins are the intracellular domain of the p75 neurotrophin receptor (p75ICD) and the C-terminal domain of the τ subunit of the *E. coli* DNA polymerase III (τ_C14). We show that 2−3 μL of 50−60 μM solutions of doubly Gd^{3+}-labeled protein can be routinely measured, featuring an order of magnitude sensitivity improvement over X-band DEER measurements. The distance distributions obtained from Gd^{3+} labeling in W-band experiments are compared with those obtained by nitroxide labeling in conventional X-band experiments, and it is shown how orientational correlation of the nitroxide radicals in the τ_C14 protein compromises data analysis at a high field. Using rotameric libraries to take the flexibilities of the tags into account, the Gd^{3+}−Gd^{3+} distance distributions measured for the two proteins are shown to be in excellent agreement with expectations based on the NMR structures of the unlabeled proteins and, in the case of p75ICD, with the metal positions determined by NMR.

Results

p75ICD. The protein p75ICD comprises residues 281−425 of the intracellular domain of the neurotrophin low-affinity receptor p75, the structure of which has been determined by solution NMR.[32] The domain contains two cysteine residues, C379 and C416, which were conjugated with nitroxide and Gd^{3+} tags. The room-temperature X-band EPR spectrum of the nitroxide labeled protein (Supporting Information (SI), Figure S1) indicated that the two nitroxide labels are highly mobile, though one less so than the other. The W-band DEER measurements of the nitroxide-labeled protein, carried out at several magnetic field positions within the EPR spectrum (inset, Figure 2a), are shown in Figure 2a. All DEER traces, except for that recorded at the highest field $A_{||}$ component, show a pronounced DEER effect where the modulations decay after the first period. In addition, the background decay is small due to the low sample concentration and the relatively small λ value. The DEER traces vary in the modulation depth because λ depends on the position of the pump pulse within the EPR spectrum. The corresponding Fourier transforms obtained after background subtraction are presented in Figure 2b. The spectra are quite similar, exhibiting singularities at the same frequencies, ±1.7 and ±2.8−3.0 MHz (shoulder), although with somewhat different relative intensities. This suggests that the orientation selection is weak. The singularities correspond to distances of 2.5 and 3.1 nm (see eq 1), in agreement with the direct extraction of the distance distribution shown in Figure 2c, obtained using Tikhonov regularization and the DeerAnalysis2008 software[14] (Figure 2b). The distance distributions obtained from the DEER traces

(23) Savitsky, A.; Dubinskii, A. A.; Flores, M.; Lubitz, W.; Möbius, K. *J. Phys. Chem. B* **2007**, *111*, 6245–6262.
(24) Marko, A.; Margraf, D.; Yu, H.; Mu, Y.; Stock, G.; Prisner, T. *J. Chem. Phys.* **2009**, *130*, 064102.
(25) Lovett, J. E.; Bowen, A. M.; Timmel, C. R.; Jones, M. W.; Dilworth, J. R.; Caprotti, D.; Bell, S. G.; Wong, L. L.; Harmer, J. *Phys. Chem. Chem, Phys.* **2009**, *11*, 6840–6848.
(26) Raitsimring, A. M.; Astashkin, A. V.; Poluektov, O. G.; Caravan, P. *Appl. Magn. Reson.* **2005**, *28*, 281–295.
(27) Abragam, A., Bleaney, B.: *Electron Paramagnetic Resonance of Transition Metal Ions*; Clarendon Press: Oxford, 1970.
(28) Raitsimring, A. M.; Gunanathan, C.; Potapov, A.; Efremenko, I.; Martin, J. M.; Milstein, D.; Goldfarb, D. *J. Am. Chem. Soc.* **2007**, *129*, 14138–14139.
(29) Potapov, A.; Song, Y.; Meade, T. J.; Goldfarb, D.; Astashkin, A. V.; Raitsimring, A. *J. Magn. Reson.* **2010**, doi: 10.1016/j.jmr.2010.03.019.
(30) Haberz, P.; Rodriguez-Castañeda, F.; Junker, J.; Becker, S.; Leonov, A.; Griesinger, C. *Org. Lett.* **2006**, *8*, 1275–1278.
(31) Su, X.-C.; Otting, G. *J. Biomol. NMR* **2010**, *46*, 101–112.
(32) Liepinsh, E.; Ilag, L.; Otting, G.; Ibañez, F. *EMBO J.* **1997**, *16*, 4999–5005.

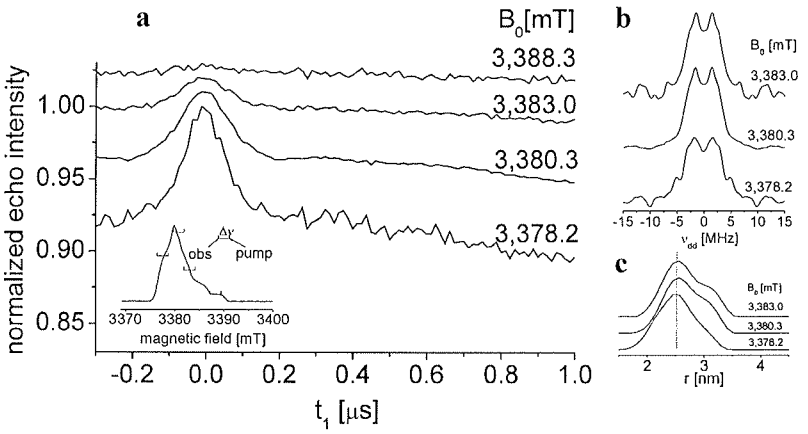

Figure 2. W-band DEER results (40 K) of doubly nitroxide-labeled p75ICD (~50 μM). (a) Raw DEER data measured at different magnetic fields. The inset shows the echo-detected EPR spectrum of this sample, indicating the positions of the pump and observe pulses. Other experimental conditions: microwave observe and pump pulses, $t_{90} = 30$ ns, $t_{180} = 60$ ns, $t_{pump} = 25$ ns, $\Delta\nu = 65$ MHz. The echo intensity scale corresponds to the 3380.3 mT trace, and all others were plotted at the same scale but shifted vertically for improved visual comparison. Measuring times were 1.5 h for the field of the maximum EPR signal and 35 h for the highest field. (b) Fourier transform of the time domain DEER data obtained after subtraction of the background. (c) Distance distribution obtained by Tikhonov regularization. Data analysis was performed using the DeerAnalysis software.[14] The vertical dotted line marks the position of the maximum of the distance distribution.

measured at 3380.3 and 3383 mT are practically the same, while that measured at 3378.2 mT has a weaker 3.1 nm shoulder. The similarity of the spectra and the distance distributions show that, in this particular case, the orientations of the two nitroxide labels are very loosely correlated and can be neglected. Therefore, the distance can be extracted directly from the time domain traces neglecting orientation selection. DEER measurements at X-band yielded a distance distribution with a maximum between 2.2 and 2.6 nm and a width of about 1 nm at half-height. The data and a comparison with the W-band results are shown in Figure S2 (SI).

To label p75ICD with Gd^{3+}, the cysteine residues were conjugated with 4-mercaptomethyldipicolinic acid (4MMDPA) or 3-mercaptodipicolinic acid (3MDPA). DPA binds lanthanides with dissociation constants in the low nanomolar range.[33] This high affinity ensures that nonspecific lanthanide binding cannot significantly compete with binding to the DPA tags. NMR spectra of p75ICD without DPA tags in the presence of Tm^{3+} showed no pseudocontact shifts, confirming the absence of natural high-affinity lanthanide binding sites.

Figure 3 shows the W-band DEER measurements obtained from 4MMDPA-Gd^{3+}- and 3MDPA-Gd^{3+}-labeled p75ICD. The absolute modulation depth is considerably lower than in the case of the nitroxide derivative because the selection of the central $|-1/2\rangle \leftrightarrow |1/2\rangle$ transition excludes all other spin states from the experiment, yielding a low λ value.[28] Nonetheless, the very intense EPR signal compensates for this, and the effective signal-to-noise ratio of the DEER effect is comparable to that obtained with the nitroxide-labeled p75ICD. The latter exhibits deeper modulation but a weaker EPR signal. Figure 3a shows the time domain DEER data with the 3MDPA labels, Figure 3b depicts the echo-detected EPR spectrum and the positions of the observe and pump pulses, and the obtained distance distribution is presented in Figure 3c, showing a maximum at 2.9 nm and a shoulder at 3.5 nm. The total width of the distance distribution (at half-height) is about 0.8 nm. The DEER data of p75ICD-4MMDPA-Gd^{3+} are shown in Figure 3d–f. Here the background decay is considerably stronger, most probably due to unbound Gd^{3+} ions arising from excess Gd^{3+} ions in solution. Nonetheless, the data show clear evidence of the first period of dipolar modulation (Figure 3a). The distance distribution has a maximum at 2.9 nm and a width of about 0.7 nm. The distance distributions for the two Gd^{3+} labels are quite broad, although the tether of 3MDPA is shorter by one CH_2 group compared to that of 4MMDPA. The maximum of the Gd^{3+}–Gd^{3+} distance distribution for either tag is about 0.4 nm longer than that of the corresponding nitroxide radicals' distance distribution, despite the similar tether lengths of MTSL and 4MMDPA. This indicates that the tags are oriented differently relative to the protein backbone.

In order to assess the metal binding sites and flexibilities of the Gd^{3+} tags, we prepared two single cysteine mutants, C379S and C416S, of p75ICD by replacing either C379 or C416 by serine and analyzed Tm^{3+} complexes of the 4MMDPA and 3MDPA derivatives by NMR spectroscopy. Different pseudocontact shifts (PCSs) were observed in ^{15}N heteronuclear single-quantum coherence (HSQC) spectra of the C379S and C416S mutants, as expected for different metal binding sites (SI Figures S3 and S4). PCSs measured with Tb^{3+}, Tm^{3+}, and Yb^{3+} complexes of the 4MMDPA derivatives (listed in Table S1, SI) were used to fit magnetic susceptibility anisotropy ($\Delta\chi$) tensors of the three lanthanides with a common metal position. In both p75ICD mutants, the metal position was found to be within 4.5–8.3 Å of the sulfur of the tagged cysteine residue, as expected for the size of the 4MMDPA tag and the uncertainty of the cysteine side-chain conformations in the NMR structure (SI Figure S5). In the case of the C379S mutant, where the tag is attached to C416, the metal position was also in close proximity of the carboxyl group of Asp397. The capacity of Asp397 to immobilize the metal ion was also indicated by the fact that very similar PCSs were observed for the 4MMDPA and 3MDPA derivatives of the C379S mutant (SI Figures S3 and S4). In contrast, the PCSs observed for the C416S mutant were less well explained by the fitted $\Delta\chi$ tensors, and the magnitudes of the apparent $\Delta\chi$ tensors were smaller (SI Table S2). This suggested partial averaging of the PCSs due to greater mobility of the tag, in agreement with the observation that the metal position found was far from any carboxyl group of the

(33) Grenthe, I. *J. Am. Chem. Soc.* **1980**, *83*, 360–364.

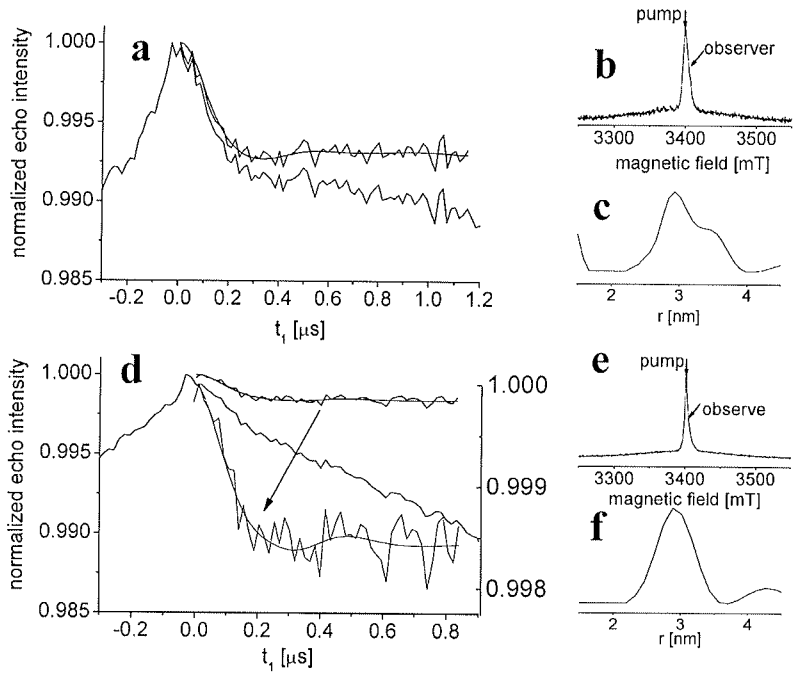

Figure 3. W-band DEER results (25 K) of p75ICD doubly labeled with either Gd^{3+}-4MMDPA or Gd^{3+}-3MDPA (~70 μM). (a) Raw DEER time domain data for p75ICD tagged with two 3MDPA-Gd^{3+}, DEER trace after subtraction of the background decay, and the corresponding superimposed calculated trace obtained with the distance distribution shown in (c). Experimental conditions: microwave observe and pump pulses, t_{90} = 12.5 ns, t_{180} = 25 ns, t_{pump} = 12.5 ns, $\Delta\nu$ = 78 MHz, and the measurement time was about 20 h. (b) Echo-detected EPR spectrum of p75ICD tagged with 3MDPA-Gd^{3+} recorded with the two-pulse echo sequence. Arrows mark the positions of pump and observe pulses. (c) Gd^{3+}−Gd^{3+} distance distribution. (d−f) Same as (a−c) except that the p75ICD was labeled with 4MMDPA-Gd^{3+}. In (d), the DEER data after subtraction of the background and the fit are also shown on the expanded scale on the right (identified by the arrow).

protein. This mutant was also much more sensitive to the identity of the tag, showing only small PCSs for the 3MDPA derivative (SI Figure S4).

^{13}C W-band electron−nuclear double resonance (ENDOR) measurements were carried out on the C379S and C416S mutants with the 4MMDPA-Gd^{3+} tag. The ENDOR spectrum of the C379S mutant, with the Gd^{3+} tag bound to C416, revealed a Gd^{3+}−^{13}C hyperfine splitting of 0.7 MHz (SI, Figure S6). This indicates coordination of the Gd^{3+} ion to a nearby protein residue, probably a carboxylate, consistent with the NMR results. For comparison, a hyperfine splitting $A_\perp$ = 0.45 MHz was obtained for ^{13}C-enriched methanol coordinated to Gd^{3+}, corresponding to a ^{13}C−Gd^{3+} distance of 0.34 nm.[34] In contrast, the ENDOR spectrum of C416S, with the 4MMDPA-Gd^{3+} tag attached to C379, showed no ^{13}C splitting (SI, Figure S6). Again, this result is consistent with the NMR results. Assuming that the 0.7 MHz splitting corresponds to $A_\perp$ and arises just from dipolar interaction, we can estimate a ^{13}C−Gd distance of 3 Å (this is a lower limit). In principle, we could select the NMR structures that are within 0.2 Å from this and display a model. However, we would rather not commit ourselves to such a model before carrying out a complete ENDOR study of the Gd^{3+} tag complex itself.

τ_C14. The protein τ_C14 contains only a single cysteine residue (C553).[35] Therefore, we designed the mutant S528C to introduce a second cysteine residue. The CW X-band EPR spectrum of the S528C mutant labeled with nitroxide radicals shows that one nitroxide label is mobile, while the other has a spectrum characteristic of a rigid nitroxide label (SI Figure S1). X-band DEER measurements performed under standard conditions where orientation selection can be ignored gave a distance distribution with a maximum at 2.5 nm and a width of about 0.7 nm (SI Figure S7). W-band DEER measurements, carried out at several magnetic field positions within the EPR spectrum (insert Figure 4a), showed a considerable DEER effect and clear modulations beyond the first period at a number of fields (Figure 4a). Unlike the case of the p75ICD, the DEER traces and the corresponding Fourier transforms obtained after background subtraction (Figure 4b) showed pronounced variations beyond the expected modulation depth, indicating a significant orientation selection. Therefore, the distance distribution cannot be readily extracted without an extensive model-dependent analysis that would have to take into account not only the distance distribution but also the distribution of five angles defining the orientation of the spin labels.[20]

The DEER measurements of τ_C14 labeled with 4MMDPA-Gd^{3+} and 3MDPA-Gd^{3+} tags are presented in Figure 5. Here the contribution of free Gd^{3+} was minimal, and the effect of the dipolar evolution is very clear also beyond the first modulation period. The distance distribution for 4MMDPA-Gd^{3+} obtained using Tikhonov regularization shows two peaks, a major one at 3.4 nm and a smaller one at 5 nm. The latter is most probably an artifact due to limitations imposed by the signal-to-noise ratio and error in the determination of background decay. This is supported by a Gaussian fit analysis that does not exhibit this distance, as shown in Figure 5. Moreover, a reliable distance determination of 5 nm requires an acquisition

(34) Raitsimring, A. M.; Astashkin, A. V.; Baute, D.; Goldfarb, D.; Poluektov, O. G.; Lowe, M. P.; Zech, S. G.; Caravan, P. *ChemPhysChem* **2006**, *7*, 1590–1597.
(35) Su, X. C.; Jergic, S.; Keniry, M. A.; Dixon, N. E.; Otting, G. *Nucleic Acids Res.* **2007**, *35*, 2825–2832.

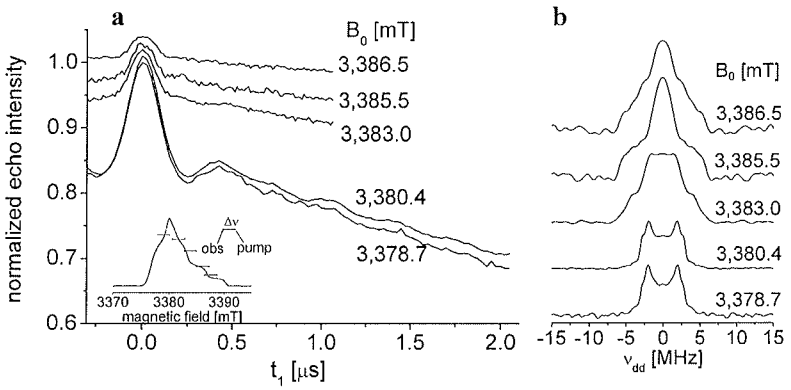

Figure 4. W-band DEER results (40 K) of doubly nitroxide-labeled τ_C14 (~60 μM). (a) DEER raw data measured at 40 K at different magnetic fields. The inset shows the field sweep echo-detected EPR spectrum of this sample at 40 K, indicating the positions of the pump and observe pulses. Experimental conditions are as in Figure 2. The measurement time was 0.5 h for the field of maximum EPR signal and 13 h at the highest field. (b) Fourier transform of the time domain DEER data obtained after subtraction of the background.

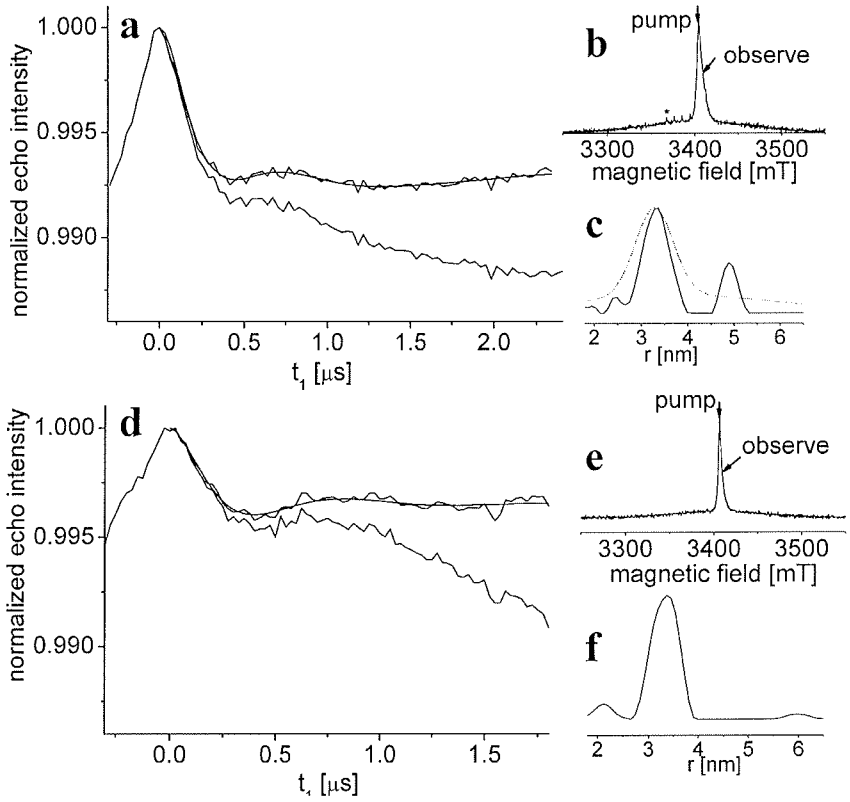

Figure 5. W-band DEER results (25 K) for τ_C14 doubly labeled with Gd^{3+}-4MMDPA and Gd^{3+}-3MDPA (~100 μM). (a) Raw DEER time domain data of τ_C14 tagged with 4MMDPA-Gd^{3+}, DEER trace after subtraction of the background decay, and the corresponding superimposed calculated trace obtained with the distance distribution shown in (c). Measurement time ~8 h. The experimental conditions were the same as in Figure 3. (b) Echo-detected EPR spectrum of τ_C14 tagged with 4MMDPA-Gd^{3+}, recorded with the two-pulse echo sequence. Arrows mark the positions of the pump and observe pulses. (c) Gd^{3+}–Gd^{3+} distance distribution. The dashed curve was obtained by a Gaussian fit. The calculated DEER trace in (a) was obtained with the Gaussian fit, and the same quality fit was obtained with the Tikhonov regularization. (d–f) Same as (a–c) except that τ_C14 was tagged with 3MDPA-Gd^{3+}.

time of 5 μs,[6] while we acquired the DEER data for only 2.2 μs. τ_C14 samples labeled with 4MMDPA-Gd^{3+} and 3MDPA-Gd^{3+} gave similar distance distributions, with a maximum at 3.4 nm and a width of ~0.8 nm (at half-height). This distance is longer than that observed for the nitroxide-labeled τ_C14 at X-band, which showed a maximum at 2.5 nm. The τ_C14 example clearly shows the advantage of the Gd^{3+} labeling over the nitroxide labeling at high fields when there is pronounced orientation selection.

Calculated Distance Distributions. To rationalize the distance distributions measured with the three types of spin labels, we calculated the distance distributions between the spin labels. This was achieved by computationally attaching to the cysteine residues in model 1 of the NMR structures (PDB codes 1NGR for p75ICD and 2AYA for τ_C14) molecular models of the spin labels with optimal bond lengths and bond angles and randomly sampling rotamer configurations of the spin label tethers.

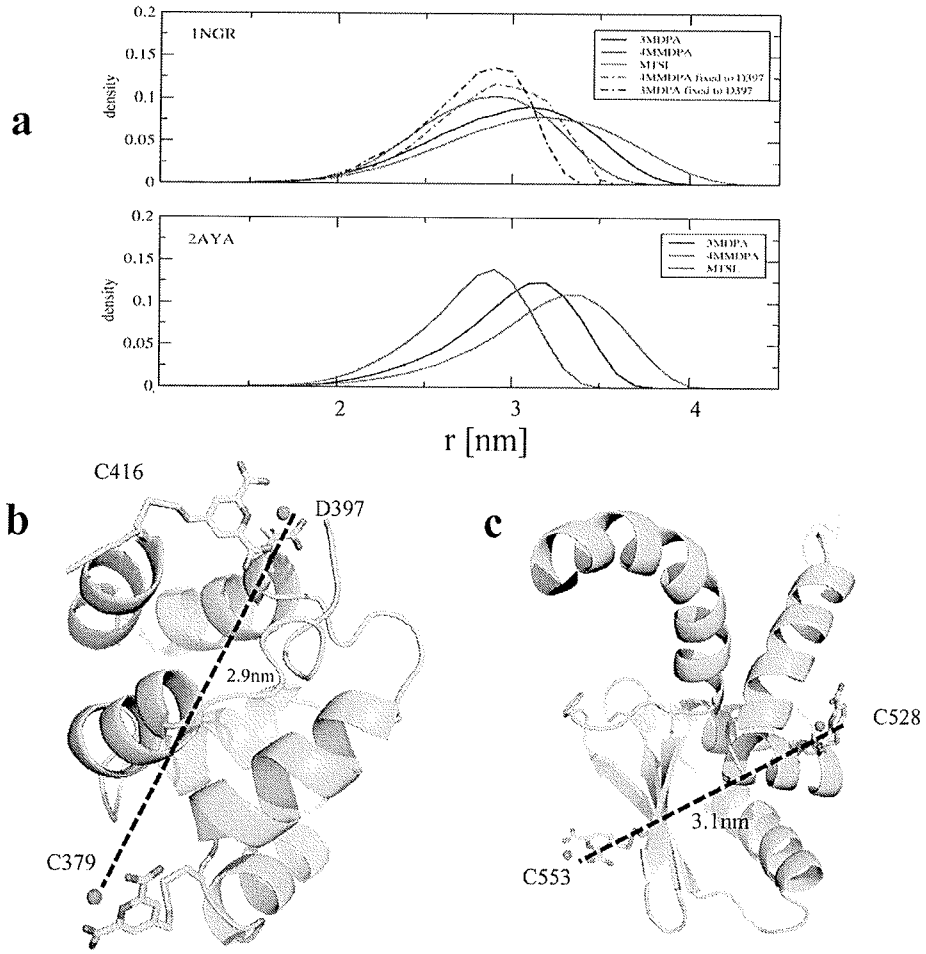

Figure 6. Distributions of Gd^{3+}–Gd^{3+} and nitrogen–nitrogen distances in p75ICD (PDB code 1NGR) and τ_C14 (PDB code 2AYA). Distances were calculated by randomly generating rotamers of the bonds connecting the paramagnetic centers with the C^α atom of the tagged cysteine residues, excluding conformations that clash with protein atoms in the NMR structures. (a) Distance distributions calculated for p75ICD. The different curves were calculated for the tags described in the figure. The dotted-dashed curves were calculated by assuming complete immobilization of one of the Gd^{3+} ions by coordination to the tag (attached to C416) and D397. Lower panel: Distance distributions calculated for τ_C14 for the tags described in the figure. (b) Cartoon of the NMR structure of p75ICD tagged with two 4MMDPA-Gd^{3+} complexes. The conformer chosen shows the Gd^{3+} ion coordinated to the tag as well as to D397. The Gd^{3+}–Gd^{3+} distance is indicated for a random conformer of the 4MMDPA tag attached to C379. (c) Cartoon of the NMR structure of τ_C14 tagged with two 3MDPA-Gd^{3+} complexes. The Gd^{3+}–Gd^{3+} distance is indicated for randomly chosen conformers of the tags attached to C528 and C553.

The results of the simulations (Figure 6) for the Gd^{3+} tags are in good agreement with the experimental distance distributions in terms of both the positions of the maxima and their widths. The maximum of the distance distribution of Gd^{3+}–Gd^{3+} ions in the samples tagged with 3MDPA is predicted to be shorter by 0.2 nm than for the samples tagged with 4MMDPA for both proteins. This small difference has not been detected experimentally. The maximum of the Gd^{3+}–Gd^{3+} distance distribution is predicted to be at 3.3 nm for τ_C14, which is close to the measured value of 3.4 nm. For p75ICD, the maximum of the calculated Gd^{3+}–Gd^{3+} distance distribution is 3.2 nm. This distance reduces to 2.9 nm when one of the Gd^{3+} ions is assumed to be immobilized by coordination to Asp397, leading to better agreement with the experimental values. Assistance by Asp397 in coordinating the Gd^{3+} ion bound to C416 is supported by the ENDOR and NMR results. The simulations show distance distributions with a width at half-height of about 0.8 nm, in close agreement with the experimental results. The width of the distance distribution is only little affected by immobilization of one of the Gd^{3+} ions. In the case of the MTSL-labeled proteins, the maximum of the calculated distance distribution (2.9 nm) was longer than the experimental value (2.5 nm) for both proteins.

Discussion

Our results demonstrate the attraction of Gd^{3+} spin labeling as a tool for nanometer-scale distance determinations in proteins by high-magnetic-field DEER measurements. The unique high-field EPR spectral properties of Gd^{3+} greatly enhance the sensitivity, correspondingly reducing the quantity of sample required. Labeled proteins at concentrations below 100 μM and in volumes of about 2 μL (corresponding to total amounts of less than 200 pmol) can be routinely measured and analyzed for distances up to 4 nm with typical measurement times of 8–12 h. Larger distances will require larger concentrations or longer accumulation times. The sensitivity is more than an order of magnitude larger compared with standard X-band DEER measurements with nitroxides. The modulation depth of DEER traces of Gd^{3+}–Gd^{3+} pairs is significantly lower than in pairs of $S = 1/2$ spins because of the low probability of finding a pair of spins with $M_S = \pm 1/2$.[28] As long as the temperature is

not too low (>10 K), the low modulation depth is partially compensated for by the intense signal of the Gd^{3+} central transition.

We also showed that excellent S/N can be obtained within 1−2 h for W-band DEER measurements of 50−100 μM and in volumes of about 2 μL of proteins doubly labeled with nitroxides when the pump pulse was set to the maximum intensity of the nitroxide spectrum (g_{yy}). Therefore, in principle, in the absence of orientation selection, W-band offers a very attractive sensitivity gain also for nitroxide labels. Unfortunately, the absence of orientational selection cannot be assumed *a priori*, and a series of measurements should be carried out to establish the lack of orientation selection, and measurements in the g_{xx} and g_{zz} regions take many hours. When orientation selection is present, as demonstrated by the results obtained with τ_C14, independent of how long the data collection is, the data analysis becomes too complicated. DEER measurements of Gd^{3+}−Gd^{3+} distances are free of this complication, and a single field measurement is sufficient, making it possible to exploit the sensitivity gain associated with high-field measurements. Therefore, Gd^{3+} spin labeling has an outstanding potential to broaden the scope of DEER applications for studies of protein structure and protein−protein interactions.

The sensitivity also depends on the width of the central Gd^{3+} transition, which in turn depends on the ZFS. Therefore, a tag inflicting a less symmetric coordination sphere on the Gd^{3+} ion would be expected to yield a broader central line and, hence, a weaker signal and a smaller λ value. We note that the λ value observed in the Gd^{3+}−Gd^{3+} DEER data (<1%) was less than expected from consideration of the line shape, the duration of the pump pulse, and the spin populations of the $|\pm 1/2\rangle$ levels. Currently we have no explanation for this. A very recent report suggests that this effect could arise from contributions of the nonsecular terms of the dipolar interaction that may be more effective for high-spin systems.[29] This has to be further verified both theoretically and experimentally.

In principle, Gd^{3+} spin labels are also effective at Q-band (34 GHz), but the sensitivity is expected to be lower due to an increased line width and significant contributions from the other transitions, which must be taken into account.[28,29] Magnetic fields much higher than W-band will be problematic, as this will lead to depopulation of the $|\pm 1/2\rangle$ levels at low temperatures. Therefore, W-band seems to be the optimal frequency. Fortuitously, W-band EPR spectrometers with sufficient power for sensitive DEER experiments with Gd^{3+} have recently become commercially available. A potential shortcoming of Gd^{3+} spin labeling, however, can be its high sensitivity to the presence of free Gd^{3+} ions in solution that enhance the background decay and can mask the DEER effect. Therefore, labeling protocols must carefully avoid the presence of free Gd^{3+} without compromising the labeling efficiency, which needs to be high in order to fully exploit the sensitivity increase offered by the method.

In addition to the sensitivity advantage of Gd^{3+}−Gd^{3+} distance measurements at high magnetic field, we were also able to predict the Gd^{3+}−Gd^{3+} distances measured for both protein examples with equal or better accuracy compared with the nitrogen−nitrogen distances between two MTSL spin labels. In both cases, the experimentally measured nitroxide−nitroxide distance distributions had a maximum at significantly shorter distances than the simulated distances (2.5 versus 2.9 nm). It is well known that nitroxide spin labels can preferentially bind to protein surfaces,[36] due to interactions with hydrophobic surface patches. We anticipate that the agreement between predicted and experimental Gd^{3+}−Gd^{3+} distances can be improved further by further immobilization of the Gd^{3+} ions with suitable linkers.[37,38] We predict that ongoing efforts to develop lanthanide binding tags for NMR applications[31,39] will further widen the scope of distance measurements by EPR in structural biology by providing ready access to accurate distance measurements in proteins, DNA, and RNA systems that currently cannot be obtained by other techniques.

Experimental Section

Protein Preparation and Labeling. p75ICD. The gene coding for residues 281−425 of the intracellular domain of the neurotrophin low-affinity receptor p75 (p75ICD) was cloned into expression plasmid pETMCSI[40] for overproduction of the protein under control of the phage T7 promoter. The 5′ primer used for PCR amplification introduced an *Nde*I site overlapping with the ATG initiation codon and an N-terminal His_6-tag. Two constructs with the single-point mutations C379S and C416S were produced by PCR amplification using mutation primers.

The wild-type protein and the two mutants C379S and C416S of p75ICD were expressed in *E. coli* strain Rosetta (λDE3)/pRARE grown in ^{15}N-autoinduction medium containing $^{15}NH_4Cl$ as the sole nitrogen source at 37 °C for 2 days. For ENDOR measurements, uniformly $^{15}N/^{13}C$-labeled samples of the C379S and C416S mutants were prepared by growing the cells overnight following induction with 1 mM IPTG at OD_{595} = 0.6.

The cells were suspended in 50 mM Tris/Cl buffer pH 7.6, 500 mM NaCl, and 2 mM dithiothreitol (DTT) and then lysed with a French press. The supernatant was collected after centrifugation and loaded on a Ni-NTA column (Pharmacia). The bound protein was eluted with an imidazole gradient from 0 to 1 M. Final yields were about 50 mg of purified p75ICD proteins per liter of culture.

Labeling of p75ICD with MTSL was performed as follows. A 0.2 mM protein solution in reaction buffer (50 mM Tris-HCl, pH 7.6) was reduced with 5 equiv of DTT, the DTT was washed out using Millipore Ultra-4 centrifugal filters (molecular weight cutoff 3000), and 30 equiv of MTSL dissolved in acetone was added stepwise to the solution and mixed well. Following stirring for 12 h at room temperature, insoluble MTSL was removed by centrifugation. The solution was washed with reaction buffer and concentrated by ultrafiltration.

The ligation of 4MMDPA or 3MDPA to C379S and C416S mutants of the p75ICD was carried out as described previously.[41,42] The ligation of 4MMDPA or 3MDPA to wild-type p75ICD was also performed as described previously,[43] except that 4 equiv of 4MMDPA or 3MDPA was used to derivatize both Cys residues with the respective tags. The samples were purified by fast protein liquid chromatography using a MonoQ column to remove residual unligated protein. The ligation efficiencies of either tag were about 80%.

For EPR measurements, 0.1 mM solutions of protein ligated with 4MMDPA or 3MDPA were prepared. The solvent was exchanged

(36) Pintacuda, G.; Otting, G. *J. Am. Chem. Soc.* **2002**, *124*, 372–373.
(37) Keizers, P. H.; Desreux, J. F.; Overhand, M.; Ubbink, M. *J. Am. Chem. Soc.* **2007**, *129*, 9292–9293.
(38) Saio, T.; Ogura, K.; Yokochi, M.; Kobashigawa, Y.; Inagaki, F. *J. Biomol. NMR* **2009**, *44*, 157–166.
(39) Otting, G. *J. Biomol. NMR* **2008**, *42*, 1–9.
(40) Neylon, C.; Brown, S. E.; Kralicek, A. V.; Miles, C. S.; Love, C. A.; Dixon, N. E. *Biochemistry* **2000**, *39*, 11989–11999.
(41) Su, X. C.; Huber, T.; Dixon, N. E.; Otting, G. *ChemBioChem* **2006**, *7*, 1599–1604.
(42) Man, B.; Su, X.-C.; Liang, H.; Simonsen, S.; Huber, T.; Messerle, B. A.; Otting, G. *Chem.—Eur. J.* **2010**, *16*, 3827–3832.
(43) Su, X. C.; Man, B.; Beeren, S.; Liang, H.; Simonsen, S.; Schmitz, C.; Huber, T.; Messerle, B. A.; Otting, G. *J. Am. Chem. So.* **2008**, *130*, 10486–10487.

to D_2O using Millipore Ultra-4 centrifugal filters (molecular weight cutoff 3000), followed by concentration to a final volume of about 80 μL. Glycerol was added to a final concentration of 20% (v/v). The final sample was obtained by adding 1.5−2 μL of a 0.45 mM solution of $GdCl_3$ to 8 μL of the protein solution such that the Gd^{3+} and 4MMDPA or 3MDPA tags were present at about equimolar ratio, leading to final concentrations of Gd^{3+} tags of about 0.06−0.07 mM.

τ_C14. A previously described[44] expression system of the gene coding for amino acid residues 499−625 of the τ subunit of *E. coli* DNA polymerase III (τ_C14) was used, directing overproduction of the protein under control of the T7 promoter in the expression plasmid pETMCSI.[40] As wild-type τ_C14 only contains a single cysteine residue (Cys553), the single-point mutation S528C was introduced by PCR amplification using mutation primers prior to protein production.

The mutant protein was produced in *E. coli* strain BL21(λDE3)*recA* in minimal M9 medium containing $^{15}NH_4Cl$ as the sole nitrogen source and purified as described.[44] The final yield of purified protein was 30 mg per liter of medium.

Labeling of τ_C14 with MTSL and ligation of 4MMDPA or 3MDPA to the S528C mutant of ^{15}N-labeled τ_C14 were performed using the same protocols as for p75ICD. The ligation efficiency was about 90%. The sample for EPR measurements was prepared as described above for p75ICD, and the final concentration of the Gd^{3+} tags was about 0.1 mM.

Fitting Metal Positions by NMR. The positions of the lanthanide ions in p75ICD-4MMDPA were determined using the PCSs observed in ^{15}N HSQC spectra of the C379S and C416S mutants with Tb^{3+}, Tm^{3+}, and Yb^{3+}. The program Numbat[45] was used to fit $\Delta\chi$ tensors to the NMR structure of the p75ICD,[32] assuming a common position for all three metal ions.

Spectroscopic Measurements. Samples for EPR measurements were prepared by mixing the solution of tagged protein (p75ICD or τ_C14) with a buffer solution containing $GdCl_3$. Quartz capillaries with 0.84 mm outer and 0.6 mm inner diameter were filled with the resulting mixture and quickly frozen in liquid nitrogen. The frozen samples were loaded into the EPR probe immersed in a liquid nitrogen bath, and the entire probe was transferred to the precooled cryostat.

W-band (95 GHz) measurements were performed on an in-house-built spectrometer.[21] All measurements of nitroxide-labeled samples were performed at 40 K and those of the Gd^{3+} labels at 25 K. Echo-detected EPR spectra were recorded with the two-pulse sequence and a delay τ of 550 ns. The "zero" dead-time four-pulse DEER sequence[7] was used for all DEER measurements. For the nitroxide samples, the separation $\Delta\nu$ between the frequencies of observation (ν_0) and pumping (ν_p) was 65 MHz, the durations of the observe $\pi/2$ and π pulses were 30 and 60 ns, respectively, and a pumping π pulse length of 25 ns was employed. For the Gd^{3+} samples, $\Delta\nu$ was 78 MHz, the durations of the observe $\pi/2$ and π pulses were 12.5 and 25 ns, respectively, and a pumping π pulse length of 12.5 ns was used. DEER measurements were also carried out with longer pump pulses to minimize the overlap between the spectral widths of the pump and observe pulses, but the results were worse. Distance distributions were derived from the dipolar time evolution data using the DeerAnalysis2008 software,[14] and Tikhonov regularization was performed with L-curve computation and the regularization parameter set to 100. When multi-Gaussian-shaped distance distribution models were assumed, the program Dfit[17] was used to analyze data. Fourier transforms were performed after subtraction of the background decay.

Calculation of Distance Distributions. First, molecular models of the spin labels were computationally attached with optimal bond length and bond angle geometries to the cysteine residues of model 1 of the NMR structures (PDB codes 1NGR for p75ICD and 2AYA for τ_C14). The conformational space available was subsequently sampled by randomly varying the dihedral angles of the four or five bonds connecting the C^α of the cysteine residue with the ring systems of the 3MDPA, 4MMDPA, and MTSL tags, keeping the rest of the protein rigid. Conformations positioning heavy atoms within 0.15 nm of each other were rejected. A total of 250 000 conformations were generated in this way for each labeled protein. Distributions of distances between the paramagnetic centers (Gd^{3+} ions in the case of 3MDPA and 4MMDPA, and the nitroxide nitrogen in the case of MTSL) were calculated by binning in intervals of 0.1 nm. For p75ICD tagged with 4MMDPA, a second set of calculations was performed assuming additional coordination of the metal ion by Asp397. In these calculations a rotamer was selected where the Gd^{3+} is positioned within 0.25 nm of both carboxyl oxygens of Asp397, and only the conformations of the second spin label were varied.

Acknowledgment. This work was supported by the Binational USA−Israel Science Foundation (D.G.) and the Australian Research Council (G.O., N.E.D., and T.H.). D.G. holds the Erich Klieger Professorial chair in Chemical Physics. D.G. thanks Arnold Raitsimring (University of Arizona) for highlighting the potential of Gd^{3+} for high-field distance measurements and for many useful discussions.

Supporting Information Available: X-band continuous-wave EPR spectra and τ_C14 DEER data of nitroxide-labeled p75ICD and ^{15}N-HSQC spectra of p75ICD mutants C379S and C416S tagged with 4MMDPA and 3MDPA, showing the PCSs obtained with Tm^{3+}; Tables of PCSs measured with Tm^{3+}, Tb^{3+}, and Yb^{3+} for the p75ICD mutants C379S and C416S with 4MMDPA, fitted $\Delta\chi$ tensors, and stereoviews of the NMR structure showing the fitted positions of the lanthanide ions. This material is available free of charge via the Internet at http://pubs.acs.org.

JA1015662

(44) Jergic, S.; Ozawa, K.; Williams, N. K.; Su, X.-C.; Scott, D. D.; Hamdan, S. M.; Crowther, J. A.; Otting, G.; Dixon, N. E. *Nucleic Acids Res.* **2007**, *35*, 2813–2824.

(45) Schmitz, C.; Stanton-Cook, M. J.; Su, X. C.; Otting, G.; Huber, T. *J. Biomol. NMR* **2008**, *41*, 179–189.